100 YEARS Journal of Ecology

British Ecological Society

Journal of Ecology doi: 10.1111/1365-2745.12515

Dynamics and persistence in a metacommunity centred on the plant *Antirrhinum majus*: theoretical predictions and an empirical test

Coline C. Jaworski*, Christophe Thébaud and Jérôme Chave

CNRS, UMR5174 Evolution et Diversité Biologique, Université Paul Sabatier, 118 route de Narbonne, 31062 Toulouse, France

Summary

1. Spatial processes have a major influence on the stability of species interaction networks and their resilience to environmental fluctuations. Here, we combine field observations and a dynamic model to understand how spatial processes may affect a network composed of the flowering plant *Antirrhinum majus*, its cohort of pollinators, and a specialist seed-predator and its parasitoid.

2. The interactions taking place within this system were investigated by determining the fate of flowers and fruits on flowering and fruiting stems at 16 study sites. We then used this information to estimate spatial and temporal variation in the pollination rate, parasitism rate and hyperparasitism rate.

3. We found that the plants were pollinator-limited, with relatively variable fruit-to-flower ratios across sites. On almost all sites, plants were both parasitized and hyperparasitized, at a low to moderate rate.

4. Comparing our field observations with a tritrophic Nicholson-Bailey model, we found that empirical data are not always consistent with the conditions for local tritrophic persistence. This suggests that other mechanisms such as random disturbances and recolonizations (patch dynamics) or inter-site migration through metacommunity dynamics (source-sink dynamics) play a role in this system. Model simulations showed that dispersal could contribute to increasing tritrophic persistence in this system, and that source-sink structure, not just environmental stochasticity, may cause the observed pattern of spatial variation.

5. *Synthesis.* We defined and measured metrics related to species interactions and densities. This led us to suggest that the functioning of the *A. majus* metacommunity is more consistent with source-sink than patch metacommunity dynamics, highlighting the extent to which dispersal explains the persistence of the system.

Key-words: biotic interactions, dispersal, patch dynamics, pollen limitation, pre-dispersal seed-predator, source-sink dynamics, species coexistence, stochasticity, tritrophic model

Introduction

Understanding and quantifying the processes by which species interaction networks are maintained across landscapes and in fluctuating environments is a critical step to implement informed conservation and management strategies (Tylianakis *et al.* 2010; Hagen *et al.* 2012; Moslonka-Lefebvre, Bonhoeffer & Alizon 2012; Pocock, Evans & Memmott 2012). Theory predicts that spatial processes play a major role in stabilizing biotic networks (Levin 1974; Hassell, Comins & May 1991; Hassell 2000; Amarasekare 2008), especially when component species occur as metapopulations and persist across habitat patches through a balance between local extinction and recolonization events (Levins 1969; Hanski & Gilpin 1991; Calcagno *et al.* 2011).

The interplay between dispersal and local community processes results in different patterns of regional species persistence (Holyoak, Leibold & Holt 2005; Logue *et al.* 2011). In the patch dynamics paradigm, the dominant process is stochastic extinction in local patches, followed by recolonization from other patches, where extinction probability is assumed to be equivalent among patches (but this assumption is easily relaxed in more general formulations). In the source-sink paradigm (mass effects), some patches are amenable to

*Correspondence author. E-mail: jaworskicoline@yahoo.fr

the stable persistence of some populations within the community and serve as sources to refill patches where local populations would otherwise not persist in the community. In the species-sorting paradigm, the local environment dominates over dispersal in shaping local communities: different species will have optimal fitness in different patches – due to local differences in selection pressure for instance – yet they may transiently persist in less suitable patches. Finally, under neutral dynamics, drift is the dominant process, affecting species extinction and recolonization rates.

These four paradigms are based on simple assumptions regarding local species interaction networks (Melián & Bascompte 2002; Amarasekare 2008), and it is unlikely that they capture the diversity of biotic interactions and spatial dynamics that take place in nature. In particular, they do not explicitly account for the widespread alterations to the landscape caused by humans (for a review, see Tscharntke *et al.* 2012). However, they have proven useful for interpreting empirical findings (Ellis, Lounibos & Holyoak 2006; Driscoll *et al.* 2010). For example, Baiser *et al.* (2013) found that local dynamics in the aquatic food web in the leaves of the pitcher plant *Sarracenia purpurea* were more rapid than dispersal, and thus patch dynamics best fitted their empirical observations. Cronin (2007) showed that planthoppers and their parasitoids present source-sink dynamics in a complex matrix. However, there have been very few field-based studies addressing the dynamics of species assemblages in a metacommunity framework (Gonzalez, Rayfield & Lindo 2011; Logue *et al.* 2011). In the archetypal example of a tritrophic network, where a prey-predator system is stabilized by introducing a natural enemy of the predator, long-term stability is difficult to infer from empirical results, but can be studied theoretically. Theoretical studies have shown, in particular, that spatial processes can alter the local dynamics (Bonsall & Hassell 2000; Holt 2002; Gouhier, Guichard & Gonzalez 2010), but also that environmental stochasticity may play a role in the stability of the network (Matias, Mouquet & Chase 2013; Ruokolainen & McCann 2013; LaBar *et al.* 2014). In order to investigate the processes that may influence the stability of biotic networks in metacommunities, it seems crucial to describe the components of such networks using empirical data, and to test their stability using a modelling framework.

In this study, we attempt to characterize the persistence of a plant/pollinator/seed-predator/parasitoid network at regional scale using natural populations of the plant *Antirrhinum majus* (snapdragon) as a study system. We used a combination of field-based estimates and a model of population dynamics to explore processes that might stabilize the *A. majus* network. We chose to study this network because it provides an excellent opportunity to investigate spatial variation in a tritrophic system. Firstly, *A. majus* is pollinated by insects (mostly bumblebees), and the rate of pollinator visits limits seed production (Tastard *et al.* 2012). Secondly, this plant produces fruiting capsules on the terminal portion of a rigid stem that persists long after fruiting and keeps the scars of the flowers that did not convert into a fruit, which serves as a measure of the overall plant-pollination success. Thirdly, the presence of seed-predators (a weevil species *Rhinusa vestita*) and of their own parasites (a parasitoid wasp) can be easily inferred from the presence and size of exit holes on the sides of the dry capsules.

Here, we first investigated the patterns of variation in biotic interactions across natural populations of *A. majus* located along an environmental gradient in the Eastern Pyrenees and then compared empirical data with simulated community dynamics to address the following questions: (i) do the fruit set and the parasitism rate (*PR*) of *A. majus* fruits by weevils vary with environmental factors across plant populations?; (ii) what are the theoretical stability conditions for our tritrophic networks locally? and (iii) which processes cause variation and persistence in empirical tritrophic networks?

Materials and methods

STUDY MODEL

Antirrhinum majus is a hermaphroditic, self-incompatible, short-lived perennial, which produces annual inflorescences with personate, zygomorphic flowers. Here, we focus on two Pyrenean subspecies of the *A. majus* complex (*A. majus* subsection *Antirrhinum sensu* Rothmaler 1956): *A. majus pseudomajus* with magenta flowers and *A. majus striatum* with yellow flowers. These subspecies are considered as sister taxa, and the main difference is flower colour (Jaworski *et al.* 2015). They occur parapatrically in the eastern part of the Pyrenees where they come into contact in a zone stretching 150 km along the Sierra del Cadi in Catalonia, Spain (Whibley *et al.* 2006; Fig. 1). Both subspecies occur from sea level to an altitude of 1900 m a.s.l. (Andalo *et al.* 2010), on limestone or siliceous substrates and in habitats with contrasting moisture regimes (rainfall 500–1000 mm per year), where they form restricted patches mostly in rocky outcrops and screes. Therefore, populations sampled along elevational gradients are likely to be confronted to very different environmental conditions, both biotic and abiotic.

Reproductive isolation in *A. majus* may be caused by the choice of pollinators (Andalo *et al.* 2010; Suchet *et al.* 2011; Tastard *et al.* 2012, 2014; Jaworski *et al.* 2015). In *Antirrhinum*, the corolla is made of two lobes that close the flower, and only large bees can access the nectar (mostly *Bombus* spp and *Xylocopa violacea*, Suchet *et al.* 2011; Tastard *et al.* 2012). Therefore, insect pollination is obligatory in this system, and fruiting is often pollinator-limited. Tastard *et al.* (2012) have carried out *in situ* manual pollen supplementation experiments in a single *A. majus* population, which was composed of hybrid plants from *A. majus pseudomajus* and *A. majus striatum*. In this natural population, fruit-to-flower ratios were 25–40%, while in the presence of pollen supplementation, this ratio increased to 80–90%. This indicates that the fruit-to-flower ratio strongly depends on pollinator availability, and that resource limitation is not a major causal factor (Holland, Bronstein & DeAngelis 2004).

Several insect herbivores feed on *Antirrhinum* including one specialist weevil, *R. vestita* (Coleoptera: Curculionidae), which is an obligate seed-predator (Caldara, Sassi & Tosevski 2010). This species has a widespread distribution in south-western Europe and is believed to have originated from France and dispersed towards Spain (Manolopoulou *et al.* 2011; Manolopoulou & Emerson 2012). Like other species in the tribe *Mecini*, weevil adult females oviposit their eggs into the flowers ovaries (Caldara, Sassi & Tosevski 2010). Larvae develop in fruits by feeding on non-mature seeds until they reach the adult

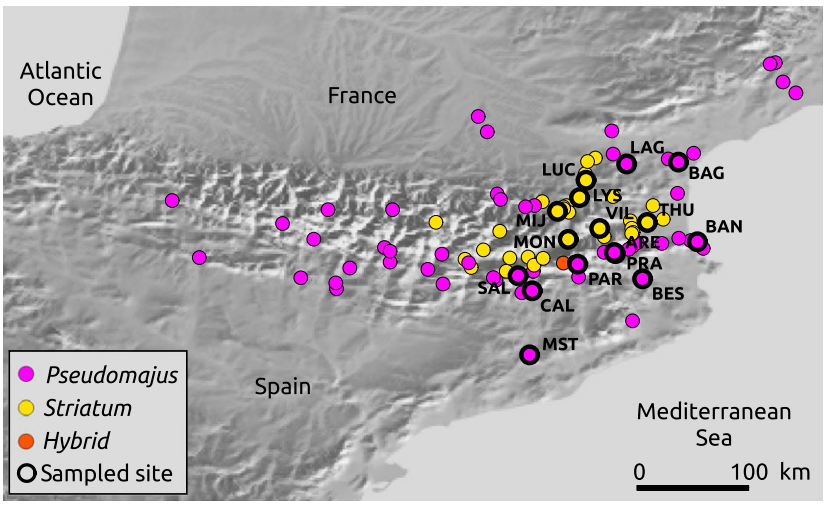

Fig. 1. Geographical distribution of *Antirrhinum majus* subspecies in the Pyrenees mountains. Localities where plant populations have been observed are illustrated by a dot (magenta: *A. majus pseudomajus*; yellow: *A. majus striatum*; orange: major hybrid zone); and no plant populations have been observed in other localities. Sites sampled in this study are illustrated by thick circles.

stage, and adults overwinter in the soil (Caldara, Sassi & Tosevski 2010). In turn, *R. vestita* weevils are often parasitized by a parasitoid wasp, which probably belongs to the *Cotesia* genus (C. Thébaud, pers. obs.).

The seeds of *A. majus* are dispersed by gravity a few metres apart when the fruit dehisces (Andalo *et al.* 2010; Khimoun *et al.* 2011), and pollen dispersal through insect pollinators is limited to a few kilometres at the very most, resulting in a degree of genetic structure among *A. majus* populations (Khimoun *et al.* 2011). Dispersal distances and dispersal rates of seed-predators and of parasitoids are unknown. Populations of *A. majus* occupy small patches (< 1 km wide in all directions) that are usually found several kilometres apart (Fig. 1), and *A. majus* plants are seldom found in isolation. Localities where *A. majus* is known to occur have been reported on Fig. 1, and intervening areas correspond to regions where the species was not found despite an exhaustive search. Moreover, plant patches are likely to be persistent (100% of 17 patches were still occupied 5 years after they were first discovered).

STUDY SITES AND SAMPLING

To explore the spatial variation of the species network, 16 *A. majus* patches, with either *pseudomajus* or *striatum* subspecies, were sampled in 2012 along an altitudinal gradient, and eight of these were resampled in 2013 (Table 1; Fig. 1). For the three trophic levels (plant, seed-predator, weevil), we assumed that each patch corresponded to a population. The size of plant populations with < 100 plants was estimated each year through exhaustive counts of plants that had flowered. The size of the larger populations (> 100 plants) was estimated through partial counts over a sub-area of the total population area. The population border was considered to have been reached when no further plants were detected within 500 m of the last plant found.

At the end of the growing season, *A. majus* plants display old floral stems that summarize the history of the biotic interactions they have experienced with their pollinators and predators. In order to characterize the plant/pollinator/seed-predator/parasitoid network, we measured up to 50 flowering plants at each study site, for each sampling season. This represented a total of 980 plants over the two sampling years. Some of the study sites were located in areas which were repeatedly disturbed by mowing or pasture (Table 1), although the variation in disturbance intensity was unknown. Plants in the disturbed sites could still produce viable seeds before being mown, and it proved to be important not to delay sampling so as to recover the plants. The impact of the disturbance level (0 for non-disturbed sites; 1 for disturbed sites, Table 1) was considered in the analyses. In practice, for the 2012 season, we sampled the populations at the end of July. In 2013, we sampled the populations 1 week later and the flowering season occurred earlier due to warm weather, thus several populations could not been recovered because the plants had already been mown. Furthermore, logistical constraints prevented us from conducting a complete census.

PLANT SCORING PROCEDURE

For each plant, we counted both mature and immature flowers and scored them (see Table S1 of Appendix S1 in Supporting Information). Mature flowers are those which have fully developed and may have formed a fruit at the date of sampling, as opposed to immature flowers (buds, opened or faded flowers). Occasionally, the plants had aborted buds or aborted fruits. These two types were also recorded, but are ignored here because they were rare (i.e. < 2% of total number of flowers; Table S1 of Appendix S1). We further classified the mature flowers either as fruiting, or as aborted flowers, when no fruit had formed but the dry sepals remained at the locus of the mature flower (Fig. 2c).

The fruits of *A. majus* are *c.* 12 mm in length, and they contain up to 300 min seeds (Andalo *et al.* 2010). These fruits were often found to be parasitized by a single (more rarely two) *Rhinusa* weevil per fruit. When a weevil has fully developed inside the fruit, it emerges by boring a large, oval hole on the side of the fruit shell, which remains empty or inhabited by the adult weevil (Fig. 2a,b). If the weevil is not yet fully developed, the larva remains in the fruit and feeds on non-mature seeds. We carefully examined each fruit and classified it as parasitized when evidence of parasitism was detected. In a few cases, the weevil larva was dead or absent, but dust from eaten seeds was taken as evidence of parasitism.

We also carefully searched for signs of hyperparasitism on each parasitized fruit. When a weevil larva is parasitized, it dies during its development within the fruit. Once the parasitoid is fully developed, it emerges by boring a small, round hole often located at the back of the fruit near the stem, surrounded by a dark circle (Fig. 2e,f). In some cases we found dead or living parasitoid wasps inside the fruit.

Thus, for each plant i, we were able to calculate the number of mature flowers f_i, the number of fruits d_i, the number of healthy fruits n_i, the number of fruits parasitized by weevils but not hyperpara-

Table 1. Description of the study sites. Sites sampled in 2012 and 2013 have two values for plant population size

Acronym	Latitude, longitude	Location	Altitude (m)	Subspecies	Plant population size	Disturbance level	Type of disturbance	Description
ARE	42.396143, 2.488232	Col d'Ares, Km 43	961	*pseudomajus*	2012: 65 2013: 63	1	Mown	Roadside bank (rocky/herbaceous)
BAG	43.107500, 2.978153	Bages	0	*pseudomajus*	2012: 175	0	Undisturbed	Dunes on seaside (rocky/herbaceous)
BAN	42.488745, 3.124752	Banyuls-sur-Mer	25	*pseudomajus*	2012: 80 2013: 20	1	Mown/ crushed	Roadside bank (rocky)
BES	42.200420, 2.699175	Besalú	155	*pseudomajus*	2012: 150	0	Undisturbed	Stone walls in village
CAL	42.107806, 1.841636	Hotel 'Cal Nen' near Berga	812	*pseudomajus*	2012: 50	1	Mown	Roadside bank (herbaceous
LAG	43.093086, 2.575092	Lagrasse, Vallée du Sou, Km 6	169	*pseudomajus*	2012: 49	1	Partially mown	Roadside bank (rocky/herbaceous)
LUC	42.966881, 2.259513	Luc-sur-Aude	225	*striatum*	2012: 30 2013: 2	1	Partially mown	Roadside bank and river-side bank (rocky)
LYS	42.831762, 2.209184	Gorges de la Pierre-Lys	375	*striatum*	2012: 60 2013: 48	1	Partially mown	Roadside bank (rocky/herbaceous)
MIJ	42.725279, 2.038218	Mijanès	1347	*striatum*	2012: 40 2013: 33	1	Partially mown	Roadside bank (herbaceous
MON	42.507516, 2.121390	Mont-Louis' citadelle	1576	*striatum*	2012: 1200 2013: 1700	1	Partially mown	Stone walls on fortifications
MST	41.609867, 1.821658	Monistrol de Montserrat	515	*pseudomajus*	2012: 16	0	Undisturbed	Roadside bank (trees/shrubs)
PAR	42.315363, 2.219561	Pardines	1098	*pseudomajus*	2012: 150	1	Mown	Roadside bank (herbaceous)
PRA	42.404787, 2.479175	Prats-de-Mollo	761	*pseudomajus*	2012: 250 2013: 200	1	Partially mown	Stone walls in village and rocky bank
SAL	42.225006 1.731879	Saldes	1216	*pseudomajus*	2012: 40	1	Grazed	Banks in pasture (herbaceous)
THU	42.638797, 2.735808	Thuir	113	*striatum*	2012: 100 2013: 89	1	Mown	Roadside bank (herbaceous)
VIL	42.591819, 2.365969	Villefranche-de-Conflent	531	*striatum*	2012: 45 2013: 31	0	Undisturbed	Bank (rocky and shrubs)

sitized s_i, and the number of hyperparasitized fruits p_i, with $d_i = n_i + s_i + p_i$. Plants with < 80% mature flowers were excluded from the analysis, in order to minimize possible bias due to phenological differences. This represented 16% of the plants.

DATA ANALYSIS

In order to study variation in pollination success across populations, we computed the fruit-to-flower ratio *K*, i.e. the ratio of the total number of fruits produced (including those which may have been parasitized and hyperparasitized), over the total number of mature flowers counted at a study site each year. We then explored the causes of variation in *K*. In a linear mixed model, the study site was specified as a random factor to correct for temporal pseudoreplication. The plant subspecies, sampling year and level of disturbance were specified as fixed-effect factors. Altitude and the log-transformed total number of mature flowers per population (as a proxy for population size; specified in Table 1) were specified as covariables in fixed effects. Starting with the most complex model with all second-order interactions between fixed effects, the most likely model was obtained by stepwise removal of effects in the model. The significance of effects was estimated through a type-II comparison of models, based on log-likelihood ratio tests. Normality was assessed using a Shapiro test on the residuals of the most likely model ($W = 0.987$, $P = 0.98$). We also computed a plant-based estimate of the fruit-to-flower ratio, as the mean ratio of the number of fruits per plant over the number of flowers per plant, and we conducted the same analysis as for the above defined community-based estimate of *K*.

In order to examine the pattern of variation in the rate of parasitism by weevils, we defined the overall *PR*, as the ratio of the total number of parasitized fruits over the total number of fruits at a study site each year. We tested for the causes in variation of *PR* using a linear mixed model, with the same fixed and random effects as for *K*, and adding *K* as a fixed effect. Due to the limitations of the data set, not all second-order interactions between fixed effects could be tested simultaneously through a type-II model comparison. Therefore, we first tested the significance of each interaction alone compared to a model including all simple effects only, and we only selected significant interactions. These were then tested simultaneously using the same method as for *K*. Normality was validated on the residuals of the most likely model (Shapiro test, $W = 0.97$, $P = 0.74$). We also computed a plant-based estimate of the *PR*, in the same way as for *K*.

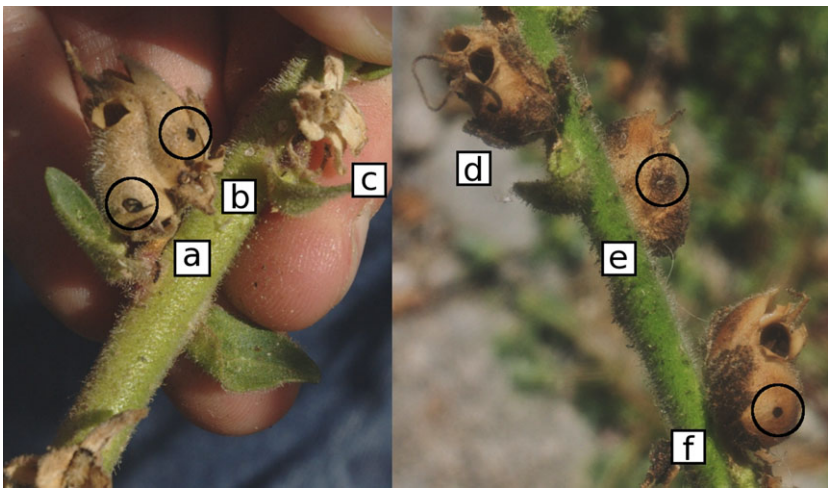

Fig. 2. Photographs of mature flowers along an *Antirrhinum majus* stem. (a, b) fruits parasitized by healthy weevils which have bored a large, oval hole on the side of the fruit shell; (c) aborted flower (dry sepals remain attached to the stem); (d) healthy fruit; (e, f) fruits hyperparasitized by healthy parasitoids which have bored a small, round hole on the side of the fruit shell.

The tests described in this section were conducted using the lme function (library nlme; Pinheiro *et al.* 2015) in the R software programme (R Development Core Team 2014).

MODELLING

Biotic interactions may cause variation in local population densities, independently of abiotic environmental factors. One approach to exploring this problem is to construct a theoretical species-interaction model, and to test whether the empirically observed variation can be expected theoretically. In other words, the present study attempts to assess whether the empirical networks are predicted to persist, under a range of scenarios. Firstly, we constructed a model that best reproduced the structure of biotic interactions in our network. Secondly, we explored the theoretical conditions of local persistence (assuming no spatial processes) in this model, and compared them with empirical observations. Thirdly, we sought to understand how spatial processes, and more precisely environmental stochasticity and dispersal, play a role in shaping the observed spatial variation and in increasing persistence in our system.

As the pollinators of our system are generalist species and do not only depend on *A. majus* flowers, mutualistic interactions were not detailed in our model. These were simply integrated by means of a global pollination rate for *A. majus* flowers. We used the classic Nicholson-Bailey system of equations to model our tritrophic network:

$$\begin{aligned} N(t+1) &= N(t).e^{r\left(1 - \frac{N(t)}{K_N}\right)}.e^{-a.S(t)} \\ S(t+1) &= N(t).\left(1 - e^{-a.S(t)}\right).e^{-b.P(t)} \\ P(t+1) &= N(t).\left(1 - e^{-a.S(t)}\right).\left(1 - e^{-b.P(t)}\right) \end{aligned} \quad (1)$$

where N, S and P are the densities of fruits escaping parasitism, seed-predators escaping hyperparasitism, and parasitoids, respectively. Parameters r and K_N are the intrinsic growth rate and the carrying capacity of the population of fruits, in the absence of predation, respectively. Thus, K_N is the theoretical maximal density of fruits in the absence of parasitism, i.e. K, the aforementioned total density of pollinated flowers. Parameters a and b are the search efficiencies of the seed-predators and the parasitoids, respectively. The escape functions $e^{-a.S(t)}$ and $e^{-b.P(t)}$ assume a random search of hosts by enemies, and a constant random search efficiency through time and space (Nicholson 1933; Nicholson & Bailey 1935; Hassell & May 1973; Beddington & Hammond 1977). This system of equations, or a modified version of these equations, is commonly used to model tritrophic interactions (Beddington & Hammond 1977; May 1978; Comins, Hassell & May 1992; Ives & Jansen 1998; Holland & DeAngelis 2001; Childs, Bonsall & Rees 2004; Satake & Bjornstad 2004; Kuang & Chesson 2008, 2010; Haque, Ali & Chakravarty 2013).

Model outputs were compared with the following empirical data:

$$N_j = \frac{\sum_{i \in Z_j} n_i}{\sum_{i \in Z_j} f_i} \; ; \; S_j = \frac{\sum_{i \in Z_j} s_i}{\sum_{i \in Z_j} f_i} \; ; \; P_j = \frac{\sum_{i \in Z_j} p_i}{\sum_{i \in Z_j} f_i} \quad (2)$$

where N_j, S_j and P_j are the empirical local densities of fruits escaping parasitism, seed-predators escaping hyperparasitism and parasitoids, at site j, respectively; Z_j is the ensemble of plants sampled at site j; and n_i, s_i, p_i and f_i are the number of healthy fruits, the number of fruits parasitized by weevils but not hyperparasitized, the number of hyperparasitized fruits, and the number of mature flowers of each plant i at site j, respectively. Hence, we assumed that healthy and dead weevils were part of a single group, and thus that weevil mortality was not due to hyperparasitism. Similarly, healthy and dead parasitoids were pooled.

LONG-TERM PERSISTENCE OF THE TRITROPHIC SYSTEM

We studied which sets of model parameters (r, a, b, K) led to system persistence, defined as the coexistence of the three species in the tritrophic network model (but in some cases, we also explored the dynamics of the plant-parasite system). It should be noted that this condition of persistence does not require that the system reaches a stable and feasible equilibrium, i.e. a stable equilibrium with all three species having a constant positive density over time (Rohr, Saavedra & Bascompte 2014), so our only requirement was that none of the three populations vanished. We first determined the persistence domain in the (r, a, b) space for $K = 0.44$, which is the mean empirical value of K across the sampled sites. We also explored how varying K led to changes in the stability domain.

The system of equations used to model our tritrophic network has no analytical solution (see the mathematical analysis in Appendix S1). We used two numerical approaches to determine a stability domain in the (r, a, b) parameter space, using $K = 0.44$. We first performed an exact linearization close to the equilibrium. We calculated the Jacobian matrix of this system of equations taken at

equilibrium (N_{eq}, S_{eq}, P_{eq}), together with its eigenvalues. For each set of (r, a, b, K), we calculated (N_{eq}, S_{eq}, P_{eq}), and we distinguished three cases: (i) non-biological or null values for (N_{eq}, S_{eq}, P_{eq}) (infeasible equilibrium *sensu* Rohr, Saavedra & Bascompte 2014); (ii) instability when the dominant eigenvalue had a modulus > 1); (iii) mathematical stability. As the conditions required for a stable and feasible equilibrium are stronger than conditions for tritrophic persistence, no continuous stable domain was obtained using the linearization method (Fig. S1 in Appendix S1). Thus, we also ran simulations for several values of (r, a, b) over 1000 time steps, from the initial densities (N_0, S_0, P_0) = (0.34, 0.057, 0.038), which correspond to the mean empirical values. We classified the regime as non-persistent if any of the (N, S, P) passed below 10^{-6} before the end of the simulation; as persistent if a non-trivial stable equilibrium point was reached, i.e. if each of the (N, S, P) converged towards positive densities; and as oscillating if the tritrophic system converged toward a cycle or a non-punctual attractor. The 10^{-6} threshold density corresponds to the extinction of a theoretical population of 10^6 individuals (i.e. about twice the number of mature flowers of the largest empirical population in our study; Table S2), assuming no effects due to small population size, such as the Allee effect (Courchamp, Clutton-Brock & Grenfell 1999). We only report herein the simulation results, the linearization analysis is included in Appendix S1 (Fig. S1). For situations where the parasitoid population was predicted to become extinct, we also conducted the stability analysis by means of simulations for a host-parasite system. The results are shown in Appendix S1 (Fig. S2).

To explore how varying K led to changes in the persistence domain, we ran simulations for K values ranging from 0 to 1. We measured the volume of the persistence domain in the (r, a, b) space as the fraction of sets of parameters (r, a, b), for which a non-trivial stable equilibrium point was reached before the end of the simulation, out of a fixed number of sets (r, a, b). For each value of K, the volume of the stability domain was expressed as a fraction of the maximal volume of persistence.

PERSISTENCE OF EMPIRICAL TRITROPHIC NETWORKS IN THE ABSENCE OF SPATIAL PROCESSES

We explored the possibility that the empirical data could be explained by the assumptions that the patches (interaction networks) are independent of each other and persistent. If the system complies with source-sink dynamics, then this hypothesis would be rejected, and we would expect to find that some sites persist in the long-term (source sites), while others do not (sink sites). We inferred the parameters (r_j, a_j, b_j) at each study site and for each year from the empirical local densities (N_j, S_j, P_j) as follows, and rewrote the system of equations of our tritrophic model at equilibrium (mathematical analysis in Appendix S1):

$$\begin{aligned} r &= \frac{-1}{1-\frac{N_{eq}}{K}}.\log\left(1-\frac{S_{eq}+P_{eq}}{N_{eq}}\right) \\ a &= \frac{-1}{S_{eq}}.\log\left(1-\frac{S_{eq}+P_{eq}}{N_{eq}}\right) \\ b &= \frac{1}{P_{eq}}.\log\left(1+\frac{P_{eq}}{S_{eq}}\right) \end{aligned} \quad (3)$$

We ran simulations for each (r_j, a_j, b_j) as described above for the exploration of the model persistence, using the local empirical pollination rate $K = K_j$ and the local threshold densities estimated as the inverse of the total number of mature flowers, measured at each site and year j (Table S2 in Appendix S1). These threshold densities allowed us to account for the impact of population size on local species persistence. We classified the regimes of the sampled sites as non-persistent, persistent or oscillating. When the regime was found to be non-persistent, we calculated the extinction time defined as the time step at which N, S or P first passed below the local threshold density. When the regime was found to be persistent, we calculated the convergence time, defined as the time step at which (N, S, P) differed from equilibrium densities by less than the local threshold density, and we also observed the behaviour of the host-parasite system (Table S2 in Appendix S1). In samples in which $P_j = 0$ (no reported parasitoid), parameter b was set to 0. In samples in which $S_j = P_j = 0$ (no reported parasite or parasitoid), we set $a_j = b_j = 0$, and the system quickly relaxed to $N_j = K$.

PERSISTENCE OF EMPIRICAL TRITROPHIC NETWORKS UNDER ENVIRONMENTAL STOCHASTICITY

An alternative explanation for the empirical patterns is that every site is a realization of the same stochastic process driven by environmental stochasticity. This hypothesis is consistent with the patch dynamics paradigm, for which each site has the same chance of disappearing from 1 year to the next, but can also be repopulated by another site. Environmental stochasticity may be defined as the temporal variation in population-level birth and death rates (Melbourne & Hastings 2008). In our model, the birth and death rates of the three species are directly linked to the parameters (r, a, b, K). Thus the variation of these parameters as calculated from empirical data provides a measure of environmental stochasticity. We used the spatial variation of these parameters observed in our empirical data as a proxy for temporal variation, and we fitted the empirical distribution of r_j, a_j, b_j and K_j with four independent normal distributions, restricting our analysis to sites where both plants and parasites were present (the outlying samples LAG_2012 and MON_2012 were also removed). We estimated the resulting mean and standard deviation values.

We explored the persistence of systems undergoing different levels of stochastic disturbance, by adding temporally uncorrelated noise to the parameters (r, a, b, K). In these simulations, new parameters (r, a, b, K) were randomly drawn at each time step from their respective zero-truncated normal distributions. We also explored the effect of reducing the variance by dividing the standard deviations by a factor of two, five and ten, as well as the impact of population size by varying the threshold density from 10^{-6} to 10^{-2}, thus encompassing the range of empirical threshold densities (Table S2 in Appendix S1). We replicated these simulations a hundred times for each combination of parameters. When the tritrophic system crashed, we calculated the extinction time in the same way as for the local persistence of the independent networks.

PERSISTENCE OF EMPIRICAL TRITROPHIC NETWORKS CONNECTED THROUGH DISPERSAL

Finally, we explored how the cross-patch dispersal of individuals at each trophic level increases the persistence of local tritrophic networks. If high dispersal rates are required to promote network persistence, this favours a source-sink metacommunity dynamics scenario. If the persistence of simulated networks in the empirical range of (r, a, b, K) parameters is low even for high inter-patch dispersal rates, this suggests the existence of other spatial processes, such as environmental niche filtering (species sorting paradigm), making some sites amenable to long-term tritrophic persistence, and some sites less amenable to persistence, irrespective of immigration rate.

We simulated a metacommunity of tritrophic networks connected through dispersal, by adding a dispersal step just after each local population dynamics step in our model:

$$\begin{array}{rcl} N(t)_{\mathrm{ad}} & = & N(t)_{\mathrm{bd}} + m_N.\left(<N(t)_{\mathrm{bd}}> - N(t)_{\mathrm{bd}}\right) \\ S(t)_{\mathrm{ad}} & = & S(t)_{\mathrm{bd}} + m_S.\left(<S(t)_{\mathrm{bd}}> - S(t)_{\mathrm{bd}}\right) \\ P(t)_{\mathrm{ad}} & = & P(t)_{\mathrm{bd}} + m_P.\left(<P(t)_{\mathrm{bd}}> - P(t)_{\mathrm{bd}}\right) \end{array} \quad (4)$$

where ad and bd mean 'after dispersal' and 'before dispersal', respectively; N, S and P are the densities of fruits escaping parasitism, weevils escaping hyperparasitism, and parasitoids, in each patch of the metacommunity, respectively; $<N>$, $<S>$ and $<P>$ are the mean densities of fruits escaping parasitism, weevils escaping hyperparasitism, and parasitoids, over all the sites in the metacommunity, respectively; and m_N, m_S, and m_P are the dispersal rates of fruits, weevils and parasitoids, respectively. Hence we considered fixed, density-independent dispersal rates, as it is typically the case in multi-patch modelling (e.g., Bonsall & Hassell 2000; Amarasekare & Nisbet 2001; Childs, Bonsall & Rees 2004; Amarasekare 2008; Gouhier, Guichard & Gonzalez 2010).

The parameters (r, a, b, K), as well as the threshold density, were randomly drawn from the empirical distributions previously defined for each patch of the metacommunity, composed of 5, 10, 15 or 20 tritrophic networks, and were set as constant over time. By doing so, we established *a priori* which patches in the metacommunity were more likely to persist, and which were more likely to be a source or a sink for each trophic level. For each number of connected patches, we varied the dispersal rate from 0 to 0.5. As seed-predators and parasitoids are likely to disperse further and at higher rates than plants, and to have similar numbers of dispersing individuals across the three trophic levels, we chose $m_S = m_P = 10{*}m_N$, based on empirical mean densities, which were one order of magnitude higher for healthy fruits than for the two higher trophic levels. We ran 500 simulations for each combination of patch number and dispersal rates, as described above. For each simulation, we calculated the proportion of patches that sustained persistent tritrophic dynamics. A patch was considered to be non-persistent if any of the three trophic levels had a null density for more than 50 time steps at the end of the simulation. We also calculated the frequency at which patches were sources, at each trophic level, as a proportion of the simulation time. A patch was considered to be a source for one trophic level at a given time step, if its density was greater than the mean density of all patches. We calculated the frequency at which a patch was source for a given trophic level, and explored how patch characteristics affected its source behaviour, by calculating correlation coefficients between the three source frequencies, the (r, a, b, K) parameters, and the threshold density. Finally, we calculated the proportion of patches that had been rescued for each trophic level at least once over the course of the simulation, i.e. patches for which the population density of the trophic level considered had dropped to zero and subsequently bounced back. In these rescued patches, we calculated the intensity of the rescue effect, as the number of times the population had been rescued. All quantities were averaged over the 500 simulations run for each combination of number of connected patches and dispersal rates.

Results

The fruit-to-flower ratio K was found to be significantly lower than one (95%-confidence interval of the intercept of the null model: [0.37; 0.50]), with a mean of 0.44 across study sites and years (Fig. 3a,b), suggesting that *A. majus* is pollinator-limited. The year of sampling had a marginal effect on K through its interaction with altitude (Fig. 3a, Table 2; K only increased with altitude in 2012), and through its interaction with the total number of flowers produced in a population (Fig. 3b, Table 2; the increase in K with the number of flowers was less pronounced in 2013 than in 2012). The plant subspecies had also a marginal effect on K, both as a single effect (Fig. 3a,b, Table 2; mean K values 0.51 and 0.38 for *A. majus striatum* and *A. majus pseudomajus*, respectively) and through its interaction with the level of disturbance (Table 2; *A. majus striatum* populations had higher K values compared to *A. majus pseudomajus* populations in non-disturbed patches only). We found similar results for our plant-based estimate of the fruit-to-flower ratio to those above using the community-based estimate of K, except that most second order interactions were significant (Subspecies * Disturbance level; Sampling year*Flower number; Sampling year*Disturbance level; Altitude*Disturbance level; Sampling year*Altitude: Flower number*Altitude; $P < 0.001$).

The *PR* was significantly affected by the interaction between population size (flower number) and altitude (Fig. 3c, Table 3). Indeed, the increase in *PR* with altitude was steeper in small populations compared to large ones. The interaction between plant subspecies and year of sampling had a marginal effect on *PR* (Fig. 3c,d, Table 3; *PR* was higher in *A. majus striatum* patches compared to *A. majus pseudomajus* patches in 2013 only). Finally, the fruit-to-flower ratio K had a marginal effect on *PR* (Fig. 3d, Table 3; *PR* decreased with K). We found similar results for our plant-based estimate of the *PR* to those above using the community-based estimate of *PR*.

We then explored whether variation in the *A. majus*/seed-predator/parasitoid network could be explained by the dynamics of species interactions, independently of abiotic factors. We first studied the theoretical conditions of persistence of a tritrophic network, and we then explored three scenarios of persistence in our empirical networks.

Assuming $K = 0.44$, the tritrophic model had a well-defined domain of persistence in the (r, a, b) parameter space, defined as the sets (r, a, b) for which a non-trivial stable equilibrium was reached before the end of the simulations (Fig. 4). The volume of this persistence domain increased sharply with K to just below $K = 0.23$, then steadily declined for higher values of K (Fig. 5). At the mean empirical value $K = 0.44$, the volume of the persistence domain was 44% of the maximal volume.

We first investigated whether local empirical densities of *A. majus* fruits, the seed-predator and its parasitoid were consistent with local persistence of the tritrophic network, assuming no migration across networks. In order to achieve this, we fitted the model parameters (r, a, b, K) for each sample and explored long-term persistence through simulations. Empirical values for K_j, (N_j, S_j, P_j) and (r_j, a_j, b_j) are provided in Table S2 (Appendix S1). Seven samples were found to lie within the persistence domain and twelve outside of it (Fig. 4). There was no correlation between extinction time and the number of mature flowers used as a proxy of population size (values are given in Table S2, Appendix S1). Out of the seven samples consistent with persistence, four were the

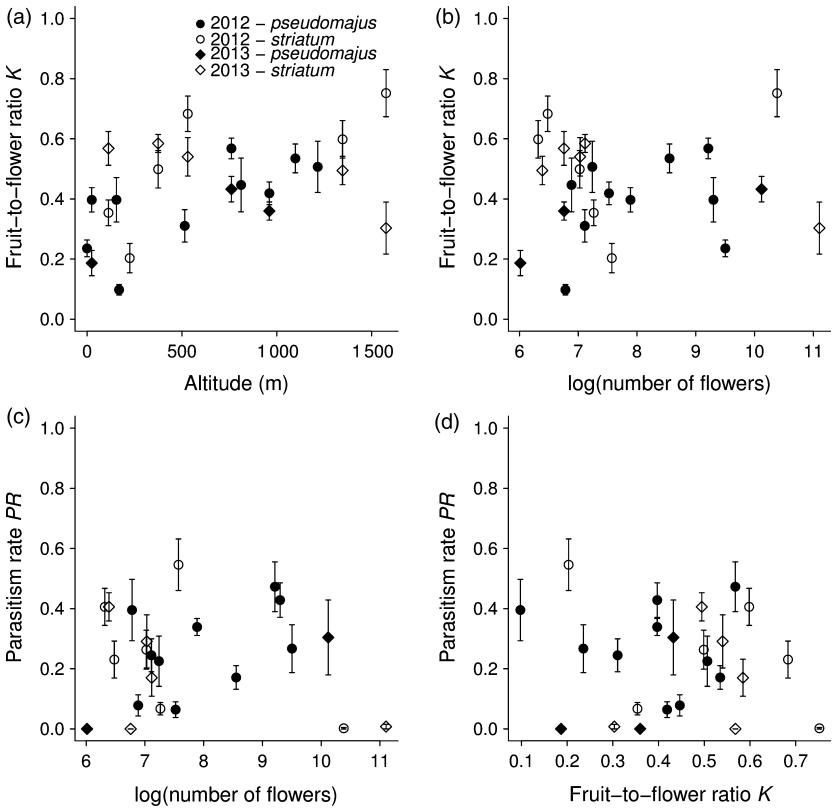

Fig. 3. Variation of the fruit-to-flower ratio K (number of fruits over number of mature flowers per study site), ±SE with respect to (a) altitude, and (b) the logarithm of the total number of mature flowers produced per population. Variation of the parasitism rate PR (number of parasitized fruits over number of fruits per study site), ±SE with respect to (c) the logarithm of the total number of mature flowers produced per population, and (d) the fruit-to-flower ratio K.

2012- and 2013-samples from sites LYS and VIL, and the remaining three were from study sites which were only sampled in 2012. When the tritrophic system did not persist, we observed numerically that the parasitoid populations became extinct first in eight of the twelve samples, whereas seed-predator and fruit populations became extinct first in two samples each. After the parasitoid population crashed, seven samples had (r, a, K) parameters consistent with persistent host-parasite dynamics (Table S2 in Appendix S1).

We then tested an alternative scenario of metacommunity persistence. We hypothesized that differences across samples may reflect the temporal stochasticity of the system and that the local networks were independently and identically distributed draws of the same regional-scale random process.

Table 2. Impact of subspecies, sampling year, disturbance level, altitude, log-transformed number of mature flowers produced in a population, and of second order interactions on the fruit-to-flower ratio K

Explanatory variable	d.f.	Log-likelihood ratio	P-value
Plant subspecies*Flower number	1	0.0140	0.91
Plant subspecies*Altitude	1	0.0382	0.85
Flower number*Disturbance level	1	0.904	0.34
Plant subspecies*Sampling year	1	3.73	0.054
Sampling year*Flower number	1	5.68	0.017*
Altitude*Disturbance level	1	2.76	0.097
Sampling year*Disturbance level	1	3.26	0.071
Plant subspecies*Disturbance level	1	4.66	0.031*
Flower number*Altitude	1	3.83	0.050
Flower number	1	0.397	0.53
Disturbance level	1	2.12	0.15
Plant subspecies	1	6.26	0.012*
Sampling year*Altitude	1	6.62	0.010*
Sampling year	1	0.0931	0.76
Altitude	1	5.78	0.056

Significance type-II tests using linear mixed models, with study sites specified as random effects, presented in order of stepwise removal from the most likely model. *P < 0.05.

Table 3. Impact of plant subspecies, sampling year, disturbance level, altitude, log-transformed number of mature flowers per population, fruit-to-flower ratio K, and of second order interactions on the parasitism rate PR.

Explanatory variable	d.f.	Log-likelihood ratio	P-value
Disturbance level	1	0.00407	0.95
Sampling year*K	1	0.119	0.73
Sampling year*Altitude	1	0.179	0.67
Subspecies*Flower number	1	0.134	0.71
Subspecies*K	1	2.49	0.11
K	1	4.61	0.032*
Plant subspecies*Sampling year	1	5.84	0.016*
Plant subspecies	1	1.88	0.17
Sampling year	1	3.00	0.084
Flower number*Altitude	1	8.90	0.0028**
Flower number	1	0.838	0.36
Altitude	1	1.21	0.27

Significance type-II tests using linear mixed models, with study sites specified as random effects, presented in order of stepwise removal from the most likely model.**P < 0.01; *P < 0.05.

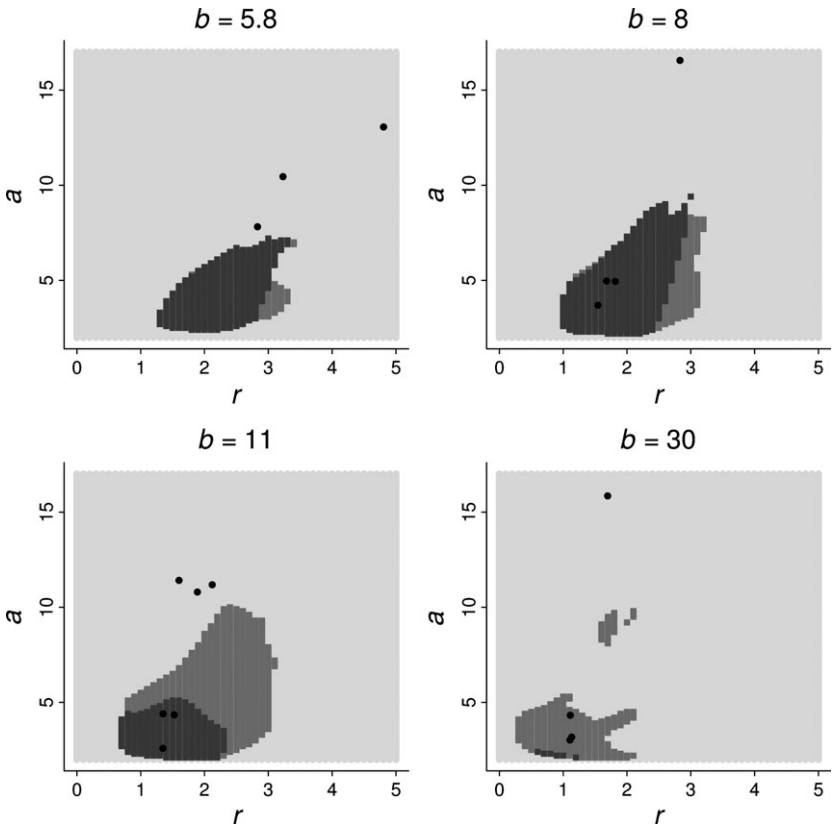

Fig. 4. Parameter space of the tritrophic model for $K = 0.44$; persistence explored through numerical simulations. Light grey domain: non-persistence, defined as the crash of one of the *N*, *S*, *P* before the end of the simulation; medium grey domain: oscillating regime, defined as the persistence of the three populations until the end of the simulation, which do not converge towards equilibrium densities; dark grey domain: persistence, defined as the convergence of the three population dynamics toward non-trivial equilibrium densities. Empirical values (black dots) are projected on the panel corresponding to the nearest value of *b*.

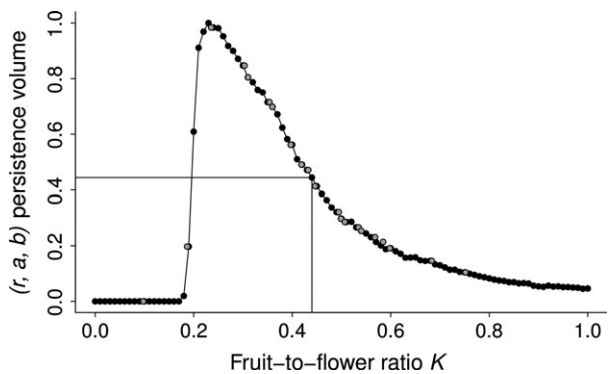

Fig. 5. Variation of the volume of the persistence domain in the (*r*, *a*, *b*) parameter space with the fruit-to-flower ratio *K*, and as a proportion of the maximal volume. Black dots: simulated volumes; grey dots: predicted volumes for the empirical *K* values; arrows: predicted volume for the mean empirical *K* value.

The multivariate normal distribution that described the empirical parameters (*r*, *a*, *b*, *K*) for this random process could be fitted to empirical data and was found to have means (1.92, 7.29, 16.1, 0.45) and standard deviations (0.92, 4.54, 13.3, 0.15). We then used random draws from this multivariate distribution to simulate tritrophic stochastic dynamics, and we found that the tritrophic system crashed in all cases. We also simulated stochastic dynamics with smaller SD values, and in this case the modelled densities (*N*, *S*, *P*) did not always match empirical ones (Fig. S3 in Appendix S1). With a low threshold density of 10^{-6} (i.e. the density under which a population went extinct), we observed a high persistence probability (> 98%) only when the standard deviation of the multivariate distribution was small (about a fifth of the empirically-measured SD; Fig. S3 in Appendix S1). With higher threshold densities, the persistence probability was smaller.

Finally, we explored how cross-patch dispersal increased persistence. We simulated sets of patches with (*r*, *a*, *b*, *K*) parameters drawn from the normal distribution calculated previously, and varied the dispersal rate and the number of patches. The proportion of persistent patches increased with both the number of connected patches, and the dispersal rate. Mean persistence increased from 20% in the absence of dispersal to over 80% for a dispersal rate of 0.1 (Fig. 6). This dispersal rate corresponded to 10% of weevils and parasitoids and 1% of fruits migrating across patches at each time step. Most local networks were alternatively source and sink independently for each trophic level, with a mean source frequency of 40%. Only 7% of the patches were source for the three trophic levels for more than half the duration of the simulation. Patches with high *K* values were often source for fruits, independently of the dispersal rate and the number of connected patches (mean correlation coefficient: 0.54). Patches with high *b* values were often sink for seed-predators, at high dispersal rates (mean correlation coefficient = −0.66 for a dispersal rate of 10%). Finally, the proportion of patches rescued was higher for parasitoid populations, up to almost 30% at the intermediate dispersal rates of 0.05 – 10% (Fig. S4 in Appendix S1). The number of patches rescued was twice and eight times smaller for seed-predator and fruit

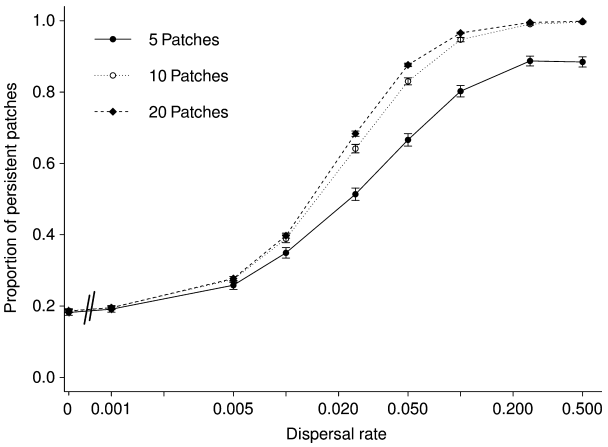

Fig. 6. Proportion of patches (mean ± SE on the 500 simulations) sustaining persistent tritrophic dynamics for different numbers of patches connected through dispersal, and under a range of dispersal rates such as $m_S = m_P = 10*m_N$, where m_N, m_S and m_P are the dispersal rates of fruits, seed-predators and parasitoids, respectively, in our tritrophic model.

populations, respectively, and slightly decreased with the number of patches connected. Patches were rescued on average 38 times over the course of the simulation, independently of the dispersal rate and the number of connected patches.

Discussion

We conducted a detailed study of biotic interactions between *A. majus*, its insect pollinators, the specialist seed-predator *R. vestita* and its parasitoid wasp. Our empirical survey suggests widespread pollinator limitation of *A. majus* plants, as shown by the low fruit-to-flower ratio, with environmental conditions having a low impact. Seed-predators and parasitoids were present in most networks both years, and the *PR* was quite variable across patches and years. An analysis of the persistence of the tritrophic model showed that not all empirical measures of the plant-insect networks were consistent with local persistence when the local networks were assumed to be independent of each other and at equilibrium. This lead us to hypothesize that inter-site differences might be due to temporal stochasticity. However, the empirically measured levels of environmental stochasticity were too high to maintain persistent dynamics in our tritrophic model. Finally, we showed that dispersal strongly increases tritrophic persistence. As is further discussed below, these findings are suggestive of source-sink metacommunity dynamics.

The relatively low fruit-to-flower ratio (44%; Fig. 3a,b) in our study was comparable to that previously measured in a plant population of *A. majus* composed of hybrids of the subspecies *striatum* and *pseudomajus* by Tastard *et al.* (2012), which was ascribed to pollinator limitation. Pollinator limitation may be associated with stochastic changes in pollinator communities, with habitat disturbance, or with other human causes (Ashman *et al.* 2004; Knight *et al.* 2005; Potts *et al.* 2010). The fruit-to-flower ratio was found to be slightly higher only at undisturbed sites of *A. majus striatum*, where plants do not frequently incur damage from human activity. This suggests that other factors, such as climatic conditions, may have limited pollination of *A. majus* plants in the studied area.

Overall, 22% of the fruits were parasitized, and seed-predators were present on most sites, both years (Fig. 3c,d, Table 2). The *PR* increased with altitude more steeply in small plant populations than in large populations. Therefore, modelling was useful for exploring the impact of population size and the interactions among species of the three trophic levels. Another possible reason for this effect is a lower hyper-*PR* in small, high-altitude plant populations, which would result in the maintaining of large seed-predator populations in the long-term, and thus in high *PR*s.

Our model helped to explore the more general problem of the persistence of *A. majus* species interaction networks, and facilitated a direct comparison with empirical population densities. Determining the conditions for mathematical stability in a dynamic model is challenging and simulations and analytical approaches sometimes yield contrasting results (Rohr, Saavedra & Bascompte 2014). Our study species reproduce yearly and synchronously, and are therefore more suitably modelled using a discrete-time model (Hassell & May 1973; Keeling, Wilson & Pacala 2002). Simulated densities may therefore undergo large changes between successive time steps, and deviate from the linear approximation. This explains why the persistence domain estimated using the simulations approach extended less into the (r, a, b) parameter space than the feasible and stable domain estimated using a linear approximation (Fig. 4 and Fig. S1 in Appendix S1). The discontinuity of the latter was due to the strong constraints of combined feasibility and mathematical stability.

Our model combined mutualistic and antagonistic interactions: the former were modelled implicitly as the carrying capacity of *A. majus* corresponded to the fruit-to-flower ratio K, which primarily depends on pollinator availability. Antagonistic interactions were modelled directly using the classic Nicholson-Bailey model, with three parameters (r, the plant growth rate; a, the *PR*; and b, the rate of parasitoid attacks). We measured the volume of the persistence domain in the (r, a, b) space as a function of the fruit-to-flower ratio K, and found a critical transition around $K = 0.23$, with non-persistence at lower K values and persistence above (Fig. 5). This showed that pollinator availability strongly influences the persistence of tritrophic interactions, and that the entire network could collapse below a certain pollinator density. This theoretical finding is consistent with results derived from a number of empirical studies (Biesmeijer *et al.* 2006), and it further supports previous findings on the risks associated with a collapse of pollinator populations (Potts *et al.* 2010). In this regards, it would be useful to compare our results with recently developed coarse-grained models of large species interaction networks (Melián *et al.* 2009; LaBar *et al.* 2014).

One of the main goals of our modelling approach was to assess the extent to which spatial processes are needed to

maintain the overall persistence of the spatial network of *A. majus*. This question has often been addressed in relation to applied management questions in agroecosystems (Thies, Roschewitz & Tscharntke 2005; Tscharntke *et al.* 2012), but the study of similar systems in the wild has provided useful insights into the processes at play (Van Nouhuys & Hanski 2002). According to the metacommunity framework, if some local populations within their community are non-persistent while other are persistent, regional persistence is only possible if the species can migrate across population patches (source-sink dynamics; Leibold *et al.* 2004; Logue *et al.* 2011). Alternatively, all local populations within the community could be equally prone to a balance between extinction and recolonization (patch dynamics). Stochastic disturbance may cause local populations to become extinct. To assess drivers of persistence in *A. majus* species networks, we first assessed whether the empirical networks were predicted to persist in the absence of dispersal and at local equilibrium. Then, we sequentially explored the influence of stochasticity and of cross-patch dispersal on persistence.

We found that only 37% of the samples had estimated (r, a, b, K) parameters compatible with persistent tritrophic dynamics in the absence of dispersal and assuming local equilibrium. At sites sampled in both years, the tritrophic dynamics were either predicted to persist both years, or to be non-persistent both years. If this pattern remains true in the long-term, this would be consistent with source-sink metacommunity dynamics, where the more persistent networks would serve as sources to refill the less persistent ones. The two sites where persistence was predicted in both years (LYS and VIL) were located at the centre of *A. majus'* range, and within valleys, facilitating migration towards neighbouring sites (Fig. 1). An explanation for the low rate of samples consistent with persistence is that local parameters (r, a, b, K) may have been improperly estimated. This has direct implications for population persistence if local dynamics are transient rather than at equilibrium, or if local dynamics vary across sites. The probability of persistence was not higher in larger plant populations, suggesting that factors other than small population size may limit persistence. In our simulations, parasitoid populations often crashed before the two other species, which concurs the theory on the determinants of food chain length (Calcagno *et al.* 2011). In practice, we found only one instance where seed-predators were reported but not parasitoids. This pattern may be explained by a higher dispersal rate of parasitoids than seed-predators, and/or different scales of other spatial processes, as has been observed in a plant/butterfly/parasitoid metacommunity (Van Nouhuys & Hanski 2002). Alternatively, parasitoids may parasitize species other than *R. vestita*, and therefore be ubiquitous in the environment, a possibility that we did not explicitly account for.

As most of the local networks were predicted to be non-persistent if considered at equilibrium and in the absence of dispersal, we explored two alternative scenarios of persistence involving spatial processes. We first explored whether environmental stochasticity alone could explain the inter-site variation observed, and assumed that all the local networks were a random draw of a single and uniform stochastic process. In this scenario, all the patches are non-persistent and would randomly go extinct if in isolation. However, they are regularly refilled from neighbouring patches. The metacommunity may persist if the mean regional (r, a, b, K) lies in the persistence domain and if the level of stochasticity is relatively small. This corresponds to the patch dynamics paradigm of metacommunity theory (Leibold *et al.* 2004; Holyoak, Leibold & Holt 2005). To test this scenario, we simulated stochastic dynamics by adding random noise to the (r, a, b, K) parameters in our model. The densities of some of the samples that were predicted to have local non-persistent dynamics were consistent with the predicted trajectories of the stochastic dynamics (Fig. S3 in Appendix S1). However, the level of environmental stochasticity predicted by the empirical data was too high to obtain persistent regional tritrophic dynamics. Other mechanisms are therefore required to maintain persistence at regional scale in a stochastic *A. majus* metacommunity, or to cause the spatial variation observed. For instance, local environmental conditions may affect persistence and induce heterogeneity among networks. In this case, depending on the relative importance of dispersal and local dynamics, we would observe source-sink dynamics or species sorting, rather than patch dynamics at the metacommunity scale. Because we used the spatial variation of (r, a, b, K) parameters to estimate stochastic temporal variation, the level of empirical stochasticity may be overestimated; a long-term study would significantly improve our estimates.

Finally, we tested a scenario of persistence where we explicitly modelled metacommunity dynamics by allowing the dispersal of individuals across patches. We showed that persistence increased significantly with dispersal in a system of connected patches within the empirical range of (r, a, b, K) parameters (Fig. 6). High dispersal rates (10% per year) were required to obtain more than 80% of persistent local networks. Persistence increased with the number of connected patches, consistent with metapopulation theory (Wilson, Hassell & Holt 1998). These results show that if empirical (r, a, b, K) parameters are considered to be fixed or slightly variable, the *A. majus* metacommunity dynamics are likely to be source-sink dynamics, where the persistence of higher trophic levels is favoured by dispersal (Leibold *et al.* 2004; Cronin 2007). If dispersal rates were smaller, this would require an alternative metacommunity structure where source patches are connected to sink patches having low extinction and colonization rates, i.e. patch dynamics with source-sink structure on a slow time scale. An empirical estimation of the extinction and colonization rates would shed light on it. The simulations showed complex source-sink dynamics, with source and sink patches varying over time and across trophic levels. This suggests a partial equivalence of patches in contributing to metacommunity dynamics, rather than a source or sink role determined by local conditions (Cronin, Haynes & Dillemuth 2004; Karban *et al.* 2012). The decoupling in source behaviour of a patch among trophic levels is likely due to the independent and random selection of parameters (r, a, b, K)

for each patch in our simulations. This may not reflect natural conditions, as some of the empirical parameters correlated (a decreased with K, and b increased with population size). Accounting more accurately for these correlations would help to characterize the *A. majus* metacommunity dynamics, which can be strongly affected by coupling across trophic levels (White 2008; White & Samhouri 2011).

By combining modelling with empirical data from an *A. majus* tritrophic network, we explored how environmental stochasticity and dispersal are likely to affect local dynamics and tritrophic persistence. If the proposed pattern of source-sink dynamics of the system is confirmed, this would imply that this system is likely to be robust to environmental changes as long as the core populations are left unaltered. In the future, this pattern of source-sink dynamics could be further tested through longer term field observations of the temporal variations in empirical parameters (r, a, b, K). This would serve to explore the impact of local environmental conditions on tritrophic persistence and on the dispersal of individuals from the three trophic levels. Field experimental studies of dispersal rates and community-wide extinction probabilities, as well as studies of the genetic structure of our three study species would also provide further insights into metacommunity dynamics. Recent studies suggest little geographical structure in *R. vestita* (Manolopoulou & Emerson 2012), and among *A. majus* populations in the Eastern Pyrenees (Khimoun *et al.* 2011), although these data alone cannot serve to infer current dispersal rates. Our findings provide a basis for assessing the underlying drivers of the eco-evolutionary dynamics of *A. majus* in the wild.

Acknowledgements

We would like to thank M. Doumeng, T. Poirier, D. Prévost and M. Vixège for their help in the field. This work was funded in part by funding from the Université Paul Sabatier. It has also benefited from "*Investissement d'Avenir*" grants managed by the French *Agence Nationale de la Recherche* (CEBA, ref. ANR-10-LABX-25-01 and TULIP, ref. ANR-10-LABX-0041).

Data accessibility

Data are archived in the appendix file Appendix S2 (see Supporting Information section).

References

Amarasekare, P. (2008) Spatial dynamics of keystone predation. *Journal of Animal Ecology*, **77**, 1306–1315.

Amarasekare, P. & Nisbet, R.M. (2001) Spatial heterogeneity, source-sink dynamics, and the local coexistence of competing species. *The American Naturalist*, **158**, 572–584.

Andalo, C., Cruzan, M., Cazettes, C., Pujol, B., Burrus, M. & Thébaud, C. (2010) Post-pollination barriers do not explain the persistence of two distinct *Antirrhinum* subspecies with parapatric distribution. *Plant Systematics and Evolution*, **286**, 223–234.

Ashman, T.-L., Knight, T.M., Steets, J.A., Amarasekare, P., Burd, M., Campbell, D.R., Dudash, M.R., Johnston, M.O., Mazer, S.J., Mitchell, R.J., Morgan, M.T. & Wilson, W.G. (2004) Pollen limitation of plant reproduction: ecological and evolutionary causes and consequences. *Ecology*, **85**, 2408–2421.

Baiser, B., Buckley, H.L., Gotelli, N.J. & Ellison, A.M. (2013) Predicting food-web structure with metacommunity models. *Oikos*, **122**, 492–506.

Beddington, J.R. & Hammond, P.S. (1977) On the dynamics of host–parasite–hyperparasite interactions. *Journal of Animal Ecology*, **46**, 811–821.

Biesmeijer, J.C., Roberts, S.P.M., Reemer, M., Ohlemüller, R., Edwards, M., Peeters, T., Schaffers, A.P., Potts, S.G., Kleukers, R., Thomas, C.D., Settele, J. & Kunin, W.E. (2006) Parallel declines in pollinators and insect-pollinated plants in Britain and the Netherlands. *Science*, **313**, 351–354.

Bonsall, M.B. & Hassell, M.P. (2000) The effects of metapopulation structure on indirect interactions in host–parasitoid assemblages. *Proceedings of the Royal Society of London. Series B, Biological Sciences*, **267**, 2207–2212.

Calcagno, V., Massol, F., Mouquet, N., Jarne, P. & David, P. (2011) Constraints on food chain length arising from regional metacommunity dynamics. *Proceedings of the Royal Society of London. Series B, Biological Sciences*, **278**, 3042–3049.

Caldara, R., Sassi, D. & Tosevski, I. (2010) Phylogeny of the weevil genus *Rhinusa* Stephens based on adult morphological characters and host plant information (Coleoptera: Curculionidae). *Zootaxa*, **2627**, 39–56.

Childs, D.Z., Bonsall, M.B. & Rees, M. (2004) Periodic local disturbance in host–parasitoid metapopulations: host suppression and parasitoid persistence. *Journal of Theoretical Biology*, **227**, 13–23.

Comins, H.N., Hassell, M.P. & May, R.M. (1992) The spatial dynamics of host-parasitoid systems. *Journal of Animal Ecology*, **61**, 735–748.

Courchamp, F., Clutton-Brock, T. & Grenfell, B. (1999) Inverse density dependence and the Allee effect. *Trends in Ecology & Evolution*, **14**, 405–410.

Cronin, J.T. (2007) From population sources to sieves: the matrix alters host-parasitoid source-sink structure. *Ecology*, **88**, 2966–2976.

Cronin, J.T., Haynes, K.J. & Dillemuth, F. (2004) Spider effects on planthopper mortality, dispersal, and spatial population dynamics. *Ecology*, **85**, 2134–2143.

Driscoll, D.A., Kirkpatrick, J.B., McQuillan, P.B. & Bonham, K.J. (2010) Classic metapopulations are rare among common beetle species from a naturally fragmented landscape. *Journal of Animal Ecology*, **79**, 294–303.

Ellis, A.M., Lounibos, L.P. & Holyoak, M. (2006) Evaluating the long-term metacommunity dynamics of tree hole mosquitoes. *Ecology*, **87**, 2582–2590.

Gonzalez, A., Rayfield, B. & Lindo, Z. (2011) The disentangled bank: how loss of habitat fragments and disassembles ecological networks. *American Journal of Botany*, **98**, 503–516.

Gouhier, T.C., Guichard, F. & Gonzalez, A. (2010) Synchrony and stability of food webs in metacommunities. *The American Naturalist*, **175**, E16–E34.

Hagen, M., Kissling, W.D., Rasmussen, C., Aguiar, M.A.D., Brown, L.E., Carstensen, D.W. *et al.* (2012) Biodiversity, species interactions and ecological networks in a fragmented world. *Advances in Ecological Research*, **46**, 89–210.

Hanski, I. & Gilpin, M. (1991) Metapopulation dynamics: brief history and conceptual domain. *Biological Journal of the Linnean Society*, **42**, 3–16.

Haque, M., Ali, N. & Chakravarty, S. (2013) Study of a tri-trophic prey-dependent food chain model of interacting populations. *Mathematical Biosciences*, **246**, 55–71.

Hassell, M.P. (2000) *The Spatial and Temporal Dynamics of Host–Parasitoid Interactions*. Oxford University Press, Oxford, UK.

Hassell, M.P., Comins, H.N. & May, R.M. (1991) Spatial structure and chaos in insect population dynamics. *Nature*, **353**, 255–258.

Hassell, M.P. & May, R.M. (1973) Stability in insect-host parasite models. *Journal of Animal Ecology*, **42**, 693–726.

Holland, J.N., Bronstein, J.L. & DeAngelis, D.L. (2004) Testing hypotheses for excess flower production and low fruit-to-flower ratios in a pollinating seed-consuming mutualism. *Oikos*, **105**, 633–640.

Holland, J.N. & DeAngelis, D.L. (2001) Population dynamics and the ecological stability of obligate pollination mutualisms. *Oecologia*, **126**, 575–586.

Holt, R.D. (2002) Food webs in space: on the interplay of dynamic instability and spatial processes. *Ecological Research*, **17**, 261–273.

Holyoak, M., Leibold, M.A. & Holt, R.D. (2005) *Metacommunities: Spatial Dynamics and Ecological Communities*. The University of Chicago Press, Chicago, IL, USA.

Ives, A.R. & Jansen, V.A.A. (1998) Complex dynamics in stochastic tritrophic models. *Ecology*, **79**, 1039–1052.

Jaworski, C.C., Andalo, C., Raynaud, C., Simon, V., Thébaud, C. & Chave, J. (2015) Learning experience influences pollinator choice for two wild *Antirrhinum majus* morphotypes. *PLoS ONE*, **10**, e0130225.

Karban, R., Grof-Tisza, P., Maron, J.L. & Holyoak, M. (2012) The importance of host plant limitation for caterpillars of an arctiid moth (*Platyprepia virginalis*) varies spatially. *Ecology*, **93**, 2216–2226.

Keeling, M.J., Wilson, H.B. & Pacala, S.W. (2002) Deterministic limits to stochastic spatial models of natural enemies. *The American Naturalist*, **159**, 57–80.

Khimoun, A., Burrus, M., Andalo, C., Liu, Z.-L., Vicédo-Cazettes, C., Thébaud, C. & Pujol, B. (2011) Locally asymmetric introgressions between

subspecies suggest circular range expansion at the *Antirrhinum majus* global scale. *Journal of Evolutionary Biology*, **24**, 1433–1441.
Knight, T.M., Steets, J.A., Vamosi, J.C., Mazer, S.J., Burd, M., Campbell, D.R., Dudash, M.R., Johnston, M.O., Mitchell, R.J. & Ashman, T.-L. (2005) Pollen limitation of plant reproduction: pattern and process. *Annual Review of Ecology, Evolution, and Systematics*, **36**, 467–497.
Kuang, J.J. & Chesson, P. (2008) Predation-competition interactions for seasonally recruiting species. *The American Naturalist*, **171**, 119–133.
Kuang, J.J. & Chesson, P. (2010) Interacting coexistence mechanisms in annual plant communities: frequency-dependent predation and the storage effect. *Theoretical Population Biology*, **77**, 56–70.
LaBar, T., Campbell, C., Yang, S., Albert, R. & Shea, K. (2014) Restoration of plant–pollinator interaction networks via species translocation. *Theoretical Biology*, **7**, 209–220.
Leibold, M.A., Holyoak, M., Mouquet, N., Amarasekare, P., Chase, J.M., Hoopes, M.F., Holt, R.D., Shurin, J.B., Law, R., Tilman, D., Loreau, M. & Gonzalez, A. (2004) The metacommunity concept: a framework for multi-scale community ecology. *Ecology Letters*, **7**, 601–613.
Levin, S.A. (1974) Dispersion and population interactions. *The American Naturalist*, **108**, 207–228.
Levins, R. (1969) Some demographic and genetic consequences of environmental heterogeneity for biological control. *Bulletin of the Entomological Society of America*, **15**, 237–240.
Logue, J.B., Mouquet, N., Peter, H. & Hillebrand, H. (2011) Empirical approaches to metacommunities: a review and comparison with theory. *Trends in Ecology & Evolution*, **26**, 482–491.
Manolopoulou, I. & Emerson, B.C. (2012) Phylogeographic ancestral inference using the coalescent model on haplotype trees. *Journal of Computational Biology*, **19**, 745–755.
Manolopoulou, I., Legarreta, L., Emerson, B.C., Brooks, S. & Tavaré, S. (2011) A Bayesian approach to phylogeographic clustering. *Interface Focus*, **1**, 909–921.
Matias, M.G., Mouquet, N. & Chase, J.M. (2013) Dispersal stochasticity mediates species richness in source-sink metacommunities. *Oikos*, **122**, 395–402.
May, R.M. (1978) Host-parasitoid systems in patchy environments – phenomenological models. *Journal of Animal Ecology*, **47**, 833–844.
Melbourne, B.A. & Hastings, A. (2008) Extinction risk depends strongly on factors contributing to stochasticity. *Nature*, **454**, 100–103.
Melián, C.J. & Bascompte, J. (2002) Food web structure and habitat loss. *Ecology Letters*, **5**, 37–46.
Melián, C.J., Bascompte, J., Jordano, P. & Krivan, V. (2009) Diversity in a complex ecological network with two interaction types. *Oikos*, **118**, 122–130.
Moslonka-Lefebvre, M., Bonhoeffer, S. & Alizon, S. (2012) Weighting for sex acts to understand the spread of STI on networks. *Journal of Theoretical Biology*, **311**, 46–53.
Nicholson, A.J. (1933) The balance of animal populations. *Journal of Animal Ecology*, **2**, 132–178.
Nicholson, A.J. & Bailey, V.A. (1935) The balance of animal populations – part I. *Proceedings of the Zoological Society of London*, **105**, 551–598.
Pinheiro, J., Bates, D., DebRoy, S. & Sarkar, D. and R Core Team (2015) *nlme: Linear and Nonlinear Mixed Effects Models*. R Package Version 3.1-122 available at http://CRAN.R-project.org/package=nlme.
Pocock, M.J.O., Evans, D.M. & Memmott, J. (2012) The robustness and restoration of a network of ecological networks. *Science*, **335**, 973–977.
Potts, S.G., Biesmeijer, J.C., Kremen, C., Neumann, P., Schweiger, O. & Kunin, W.E. (2010) Global pollinator declines: trends, impacts and drivers. *Trends in Ecology & Evolution*, **25**, 345–353.
R Development Core Team (2014) *R: A Language and Environment for Statistical Computing*. R Foundation for statistical computing, Austria, Vienna.
Rohr, R.P., Saavedra, S. & Bascompte, J. (2014) On the structural stability of mutualistic systems. *Science*, **345**, doi: 10.1126/science.1253497.
Rothmaler, W. (1956) *Taxonomische Monographie der Gattung Antirrhinum*. Akademie-Verlag, Berlin, Germany.
Ruokolainen, L. & McCann, K. (2013) Environmental weakening of trophic interactions drives stability in stochastic food webs. *Journal of Theoretical Biology*, **339**, 36–46.
Satake, A. & Bjornstad, O.N. (2004) Spatial dynamics of specialist seed predators on synchronized and intermittent seed production of host plants. *The American Naturalist*, **163**, 591–605.
Suchet, C., Dormont, L., Schatz, B., Giurfa, M., Simon, V., Raynaud, C. & Chave, J. (2011) Floral scent variation in two *Antirrhinum majus* subspecies influences the choice of naïve bumblebees. *Behavioral Ecology and Sociobiology*, **65**, 1015–1027.
Tastard, E., Ferdy, J., Burrus, M., Thébaud, C. & Andalo, C. (2012) Patterns of floral colour neighbourhood and their effects on female reproductive success in an *Antirrhinum* hybrid zone. *Journal of Evolutionary Biology*, **25**, 388–399.
Tastard, E., Andalo, C., Burrus, M., Gigord, L. & Thébaud, C. (2014) Effects of floral diversity and pollinator behaviour on the persistence of hybrid zones between plants sharing pollinators. *Plant Ecology & Diversity*, **7**, 391–400.
Thies, C., Roschewitz, I. & Tscharntke, T. (2005) The landscape context of cereal aphid–parasitoid interactions. *Proceedings of the Royal Society of London. Series B, Biological Sciences*, **272**, 203–210.
Tscharntke, T., Tylianakis, J.M., Rand, T.A., Didham, R.K., Fahrig, L., Batáry, P. *et al.* (2012) Landscape moderation of biodiversity patterns and processes – eight hypotheses. *Biological Reviews*, **87**, 661–685.
Tylianakis, J.M., Laliberté, E., Nielsen, A. & Bascompte, J. (2010) Conservation of species interaction networks. *Biological Conservation*, **143**, 2270–2279.
Van Nouhuys, S. & Hanski, I. (2002) Colonization rates and distances of a host butterfly and two specific parasitoids in a fragmented landscape. *Journal of Animal Ecology*, **71**, 639–650.
Whibley, A.C., Langlade, N.B., Andalo, C., Hanna, A.I., Bangham, A., Thébaud, C. & Coen, E. (2006) Evolutionary paths underlying flower color variation in *Antirrhinum*. *Science*, **313**, 963–966.
White, J.W. (2008) Spatially coupled larval supply of marine predators and their prey alters the predictions of metapopulation models. *The American Naturalist*, **171**, E179–E194.
White, J.W. & Samhouri, J.F. (2011) Oceanographic coupling across three trophic levels shapes source-sink dynamics in marine metacommunities. *Oikos*, **120**, 1151–1164.
Wilson, H.B., Hassell, M.P. & Holt, R.D. (1998) Persistence and area effects in a stochastic tritrophic model. *The American Naturalist*, **151**, 587–595.

Received 21 October 2014; accepted 16 November 2015
Handling Editor: Caroline Brophy

Supporting Information

Additional Supporting Information may be found in the online version of this article:

Appendix S1. Mathematical complements, simulation results and supplementary information on the study sites.

Appendix S2. Empirical data used in the study.